Chinese Chemical Letters 35 (2024) 108487

Contents lists available at ScienceDirect

Chinese Chemical Letters

journal homepage: www.elsevier.com/locate/cclet

Constructing high-capacity and flexible aqueous zinc-ion batteries with air-recharging capability using organic cathodes

Xiaojuan Chen[a,1], Haoqi Su[a,1], Baozhu Yang[a], Xiaocen Liu[a], Xiuting Song[a], Lixin Su[a], Gui Yin[b], Qi Liu[a,b,*]

[a] *Jiangsu Key Laboratory of Advanced Catalytic Materials and Technology, Advanced Catalysis Green Manufacturing Collaborative Innovation Center and School of Petrochemical Engineering, Changzhou University, Changzhou 213164, China*
[b] *State Key Laboratory of Coordination Chemistry, Nanjing University, Nanjing 210093, China*

ARTICLE INFO

Article history:
Received 8 March 2023
Revised 30 March 2023
Accepted 20 April 2023
Available online 23 April 2023

Keywords:
Aqueous zinc-ion battery
Trinitrohexaazatrinaphthylene
Organic cathode materials
Flexible air-rechargeable battery
Self-powered system

ABSTRACT

Flexible aqueous zinc-ion batteries (AZIBs) with air-recharging capability are a promising self-powered system applied in future wearable electronics. It is desired to develop high-capacity air-rechargeable AZIBs. Herein, we developed a flexible AZIB with air-recharging capability based on trinitrohexaazatrinaphthylene (TNHATN) cathode and a $ZnSO_4$ electrolyte. The flexible Zn//TNHATN battery exhibits high volumetric energy density (21.36 mWh/cm^3) and excellent mechanical flexibility. Impressing, the discharged flexible Zn//TNHATN battery can be chemical self-charged *via* the redox reaction between TNHATN cathode and O_2 from the air. After oxidation in air for 15 h, such flexible Zn//TNHATN battery can deliver a high specific capacity of 320 mAh/g at 0.5 A/g, displaying excellent air-recharging capability. Notably, this flexible Zn//TNHATN battery also works well in chemical or/and galvanostatic charging mixed modes, showing reusability. This work provides a new insight for designing flexible aqueous self-powered systems.

Aqueous zinc-ion batteries (AZIBs) with low cost and high safety have received considerable attention for their potential application in large-scale energy storage and wearable electronics [1–12]. In general, the recharge of AZIBs needs using external electricity power. But, the recharge of AZIBs will be restricted in some outdoors circumstances where the electrical energy cannot be provided. To overcome this limitation, numerous self-charging power systems were invented and created to extract energy from renewable resources, such as sunlight, wind energy and air [13,14]. It is a pity that sunlight and wind energy are not available anytime and anywhere. In contrast, air can provide cost-free energy resources anytime and anywhere through oxygen, because the chemical energy of oxygen molecules can be converted into electrical energy *via* redox reactions [15]. Recently, AZIBs with air-recharging capability have begun to be reported [16–21], but, they are still in their infancy and some of them also faced with problems of low air-recharging capability and capacity improvement. So, developing new AZIBs with excellent air-recharging capability, high capacity and high stability is still an important task. To achieve this goal, selection of cathode materials is very critical, due to the potential difference between discharged cathodes and O_2 is relative to the air-recharging capability for AZIBs. Compared with inorganic compounds, organic compounds as electrode materials have advantages of structural designability, sustainability and controllable synthesis [22,23]. Various organic aromatic compounds containing carbonyl/imine groups (C=O/C=N) as the cathode materials of AZIBs have been developed in recent years, owing to carbonyl/imine groups can coordinate reversibly and efficiently with Zn^{2+}/H^+ ions [24–37]. Very recently, Niu *et al.* reported an air-rechargeable Zn/organic battery with H^+-based chemistry, displaying an application promising of organic cathode in self-powered systems [21]. On the other hand, we have found that it is an effective route to introduce electron-withdrawing groups into π-conjugated aromatic molecule for obtaining high-performance organic cathode materials of AZIBs [35]; besides, we also noted that nitro group (-NO_2) is not only an electron-withdrawing group, but also can coordinate with Li^+ ions [38]. Inspired by these facts, we synthesized a new π-conjugated aromatic compound trinitrohexaazatrinaphthylene (TNHATN) with both multiple redox active

* Corresponding author at: Jiangsu Key Laboratory of Advanced Catalytic Materials and Technology, Advanced Catalysis Green Manufacturing Collaborative Innovation Center and School of Petrochemical Engineering, Changzhou University, Changzhou 213164, China.
E-mail address: liuqi@cczu.edu.cn (Q. Liu).
[1] These authors contributed equally to this work.

https://doi.org/10.1016/j.cclet.2023.108487
1001-8417/

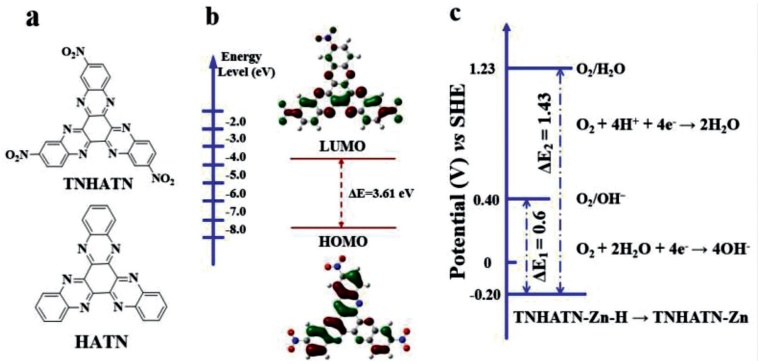

Fig. 1. (a) Molecular structures of TNHATN and HATN. (b) LUMO/HOMO energy levels of TNHATN, as well as optimized structures of the molecule used in the study obtained using the DFT method. (c) Energy level transition diagram for TNHATN-Zn-H and O_2.

sites (C=N and -NO_2 groups) *via* introducing electron-withdrawing groups (-NO_2) into hexaazatrinaphthylene (HATN) (Fig. 1a), and developed an air-rechargeable AZIB based on TNHATN cathode. Impressively, the discharged TNHATN cathode (TNHATN-Zn-H) can be converted to the charged state *via* the spontaneous redox reaction with O_2 in air, due to the potential difference between TNHATN-Zn-H and O_2 (Fig. 1c), thus, when worked open to the air, the discharged flexible aqueous Zn//TNHATN battery can be chemically self-recharged *via* O_2 from air.

TNHATN can be synthesized by the condensation reaction of 4-nitro-*o*-phenylenediamine and hexaketocyclohexane, as displayed in Scheme S1. The solid-state ^{1}H NMR (^{1}H SSNMR), solid-state ^{13}C NMR (^{13}C SSNMR), FT-IR, XRD spectra and FESEM images of as-synthesized TNHATN shown in Figs. S1-S4 (Supporting information) demonstrate its chemical structure, high purity, crystalline, and morphology of micron-scaled particles.

The lowest unoccupied molecular orbital (LUMO) energy level (-3.83 eV) of TNHATN molecule is lower than that (-2.62 eV) of HATN (Fig. 1b) [32]. The lower the LUMO energy level means that TNHATN molecule possesses the stronger electron affinity and the higher discharge potential [30]. The smaller energy band gap (E_g) for the TNHATN molecule (3.61 eV) is associated with its N-containing π-conjugated aromatic structure [39], which is favorable to the enhancement of its electrochemical performance.

Considering one -NO_2 group can obtain two electrons to the maximum extent [38], then, one TNHATN should obtain 12 electrons in theory, its theoretical specific capacity can reach at 620 mAh/g, higher than that of HATN (418 mAh/g). So, it is promising that TNHATN compound is used as a cathode material for AZIBs.

Aqueous Zn//TNHATN coin-type batteries were used to investigate the electrochemical performances of TNHATN as the cathode. Each cyclic voltammetry (CV) curve of the Zn//TNHATN battery (Fig. 2a) has two obvious reduction peaks at around 1.18 and 0.23 V, two weaker reduction peaks at around 0.62 and 0.42 V, and two oxidation peaks at around 0.56 and 1.22 V. The production of these redox peaks might be ascribed to the uptake/removal of Zn^{2+} and H^+ ions [32,40]. With the scan rate increases from 0.1 mV/s to 0.5 mV/s, because of the polarization increasing, the potential of reduction/oxidation peak moves toward the negative/positive direction. The linear curves produced from the expression ($i = av^b$) are displayed in Fig. 2b, in which *v, i, a* and *b* stand for scan rate (mV/s) and peak current (mA), constant, respectively [41]. The *b* values of four peaks are 0.63, 0.64, 0.87 and 0.73, respectively, indicating the combined effect of capacitive behavior and ionic diffusion [18]. As the scanning rate increased from 0.1 mV/s to 0.5 mV/s, the contribution for capacitive controlled process gradually changed from 46.1% to 64.9% (Fig. S5 in Supporting information), indicating that the capacitive controlled process is dominant at 0.5 mV/s for the energy storage behaviors of the Zn//TNHATN battery.

The galvanostatic discharge/charge curves for the Zn//TNHATN battery at a low current density of 0.04 A/g is shown in Fig. 2c. It can be seen from Fig. 2c that the first discharge specific capacity is high up to 3246 mAh/g, while the first charge specific capacity has only 978 mAh/g, showing an obviously irreversible capacity loss (according to the mass of TNHATN in cathode, the capacities were calculated). Similar phenomenon also exists in the second, third, fourth and fifth cycles, which might be attributed to the formation of by-products, such as $Zn_4(OH)_6SO_4{\cdot}5H_2O$, and the reduction of dissolved O_2 [31,32,42]. Notably, the fourth and fifth discharge specific capacities still maintain at 1115 and 414 mAh/g, respectively (Fig. 2c and Fig. S6 in Supporting information), outperforming the values of many organic cathodes in AZIBs reported (Table S1 in Supporting information). But, the capacity of 414 mAh/g is lower than its theoretical specific capacity. As shown in Fig. 2d, at a current density of 0.1 A/g, there are two inconspicuous platforms in the discharge/charge curve, corresponding to the TNHATN electrode happens multiple redox reactions, as revealed in the CV curve with multiple redox peaks (Fig. 2a). When the current density increases to 0.1, 0.5, 1, 2, 5, 10 and 20 A/g, the Zn//TNHATN battery keeps the average discharge specific capacity of 363, 299, 279, 264, 252, 241 and 239 mAh/g, respectively, exhibiting a good rate capability (Fig. 2d and Fig. S6). As the current density returns to 0.04, 0.1 and 0.5 A/g, the average discharge specific capacity of 435, 309, 269 mAh/g can be restored, respectively, revealing the TNHATN electrode has the better electrochemical reversibility (Fig. S6). This good electrochemical reversibility is further verified by the successive five almost overlap CV curves of the Zn//TNHATN battery at 0.5 mV/s shown in Fig. S7 (Supporting information). It is worth mention that at the high current density of 20 A/g, the Zn//TNHATN battery displays a high rate performance similar to a supercapacitor, because it can finish a discharge process of 239 mAh/g capacity within 42 s.

The cycling characteristics of the TNHATN electrode was also investigated (Fig. 2e). At a current density of 5 A/g, the Zn//TNHATN battery delivers a specific capacity of 251 mAh/g in the first discharge process, and still remains the capacity of 169 mAh/g after 1000 cycles. The capacity retention of 67.3% and the Coulombic efficiency of almost 100% demonstrate the TNHATN electrode has the better long cycling stability. For the TNHATN electrode, the average irreversible capacity loss (ICL) was calculated to be 0.033% during 1000 cycles. Such high discharge capacity (251 mAh/g) at 5 A/g is higher or comparable to that of the reported organic compounds used in AZIBs as the cathode materials [29–31]. The stability of the TNHATN electrode was also demonstrated by the self-discharge tests results of Zn//TNHATN batteries (Fig. S8 in Supporting information).

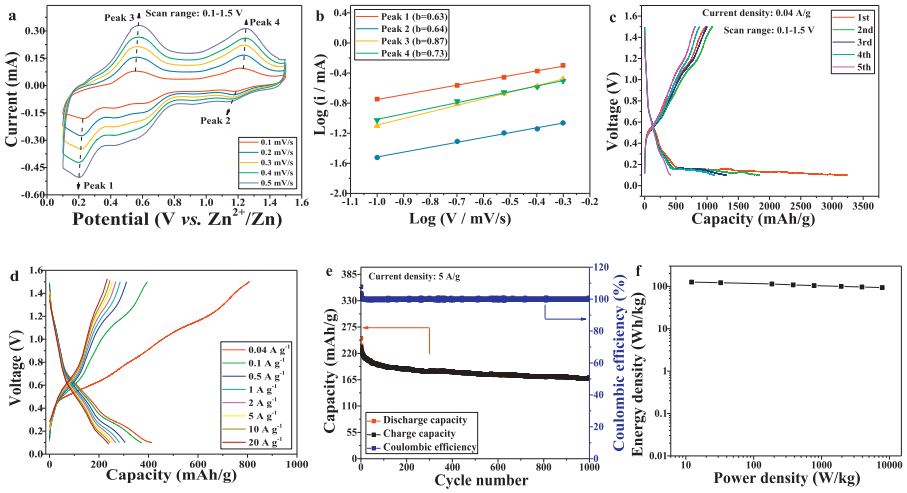

Fig. 2. Electrochemical performances of aqueous Zn//TNHATN batteries (a) CV curves at various scanning rates of 0.1 mV/s to 0.5 mV/s. (b) log(i)~log(v) plots of the redox peaks originate from the CV curves. Discharge-charge curves (c) at a low current density of 0.04 A/g and (d) at different current density within 0.1–1.5 V. (e) Cycle stability at a current density of 5 A/g and (f) the energy density and power density of aqueous Zn//TNHATN battery.

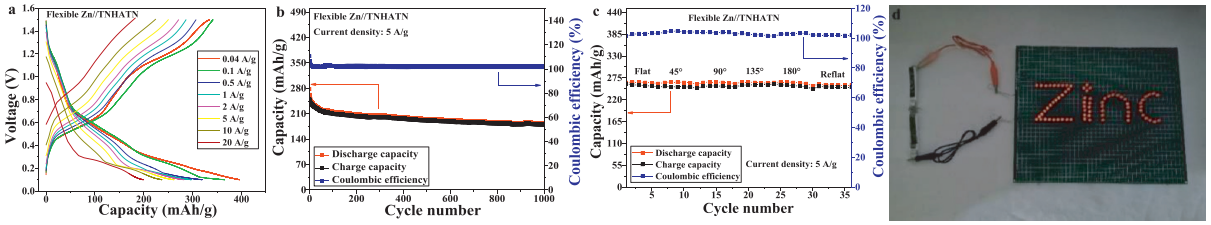

Fig. 3. (a) Galvanostatic charge-discharge curves of flexible aqueous Zn//TNHATN battery at different current densities within 0.1–1.5 V. (b) Cycle performance. (c) Cycle stability of the flexible aqueous Zn//TNHATN battery at 5 A/g at various folding angles. (d) Photograph of lightening 74 LED lights using two such batteries.

According to the charge-discharge data presented in Fig. 2d and the total mass of the active organic material and the consumed Zn, the energy density and power density of the Zn//TNHATN battery can be calculated (see Supporting information for detail calculation). The energy density of the Zn//TNHATN battery is 126 Wh/kg when the power density is 12.2 W/kg (Fig. 2f), which is comparable to that of many reported AZIBs [29–31]. Along with the power density increases to 7.8 kW/kg, the energy densities can keep at 93.5 Wh/kg. Besides, with the TNHATN loading increase, the specific capacity decreases (Fig. S9 in Supporting information), owing to the resistances of organic materials increase. Despite all this, using this organic material in grid-scale energy storage systems is also attractive, considering the rich source of organic materials. The electrochemical reaction mechanism of TNHATN involving co-insertion/co-removal of Zn^{2+} and H^{+} ions have been verified by ^{1}H SSNMR, ^{13}C SSNMR, FT-IR, XRD spectra, SEM-EDS, CV curves analysis and DFT calcualtion (Figs. S10–S16 in Supporting information), which can be simply expressed as follows:

$$\text{TNHATN} \underset{-12e^{-},\,-nZn^{2+},\,-(12-2n)H^{+}}{\overset{+12e^{-},\,+nZn^{2+},\,+(12-2n)H^{+}}{\rightleftharpoons}} \text{TNHATN - nZn - (12-2n)H} \quad (1)$$

The flexible aqueous Zn//TNHATN batteries assembled were used to evaluate the potential application of TNHATN in the wearable electronics (see Fig. S17 and the experimental details in Supporting information). As depicted in Fig. 3a and Fig. S18a (Supporting information), the flexible aqueous Zn//TNHATN battery can provide a high discharge specific capacity of 755 mAh/g when it first discharges at 0.04 A/g, and the average discharge capacity is 503 mAh/g for five cycles (Fig. S18b in Supporting information). As the current density raises to 0.1, 0.5, 1, 2, 5, 10 and 20 A/g, the corresponding average discharge specific capacities are 352, 312, 295, 280, 256, 231 and 184 mAh/g, respectively, presenting similar high-rate performance with the Zn//TNHATN coin-type batteries. Along with the current density is back to 0.04 and 0.1 A/g, the discharge specific capacities can return to 302 and 280 mAh/g, respectively, showing the flexible aqueous Zn//TNHATN battery has good reversibility.

We also investigated the long cycle stability of flexible aqueous Zn//TNHATN batteries. As shown in Fig. 3b, the initial discharge capacity at 5 A/g is 277 mAh/g, and after 1000 cycles, the flexible aqueous Zn//TNHATN battery can still provide a specific capacity of 182 mAh/g, maintaining 100% Coulombic efficiency and about 71% capacity retention, showing good cycle stability. The Ragone plot based on above data is displayed in Fig. S19 (Supporting information), which reflects the relation between the volumetric energy density and power density for the flexible battery (see calculation details in Supporting information). The maximum volumetric energy density of flexible aqueous Zn//TNHATN batteries is 21.36 mWh/cm^3, which is superior to many previously reported flexible batteries and supercapacitors. (Table S3 in Supporting information). The excellent electrochemical performances of the Zn//TNHATN battery is related with following factors: (1) TNHATN compound has a π-conjugated aromatic structure containing multiple redox active sites (C=N and -NO_2 groups) and electron-withdrawing groups (-NO_2). (2) TNHATN compound is difficult to dissolve in the electrolyte.

To research the flexibility of the flexible aqueous Zn//TNHATN battery, we tested the cycling stability of it at flat, 45°, 90°, 135°, 180° and reflat (Fig. 3c and Fig. S20 in Supporting information). At a current density of 5 A/g, the battery cycled for 6 times at each folding angle, and after a series of angle folding, the TNHATN electrode can still keep a capacity of 256 mAh/g (97% of the initial capacity) when it returns to the flat state. Compared the dis-

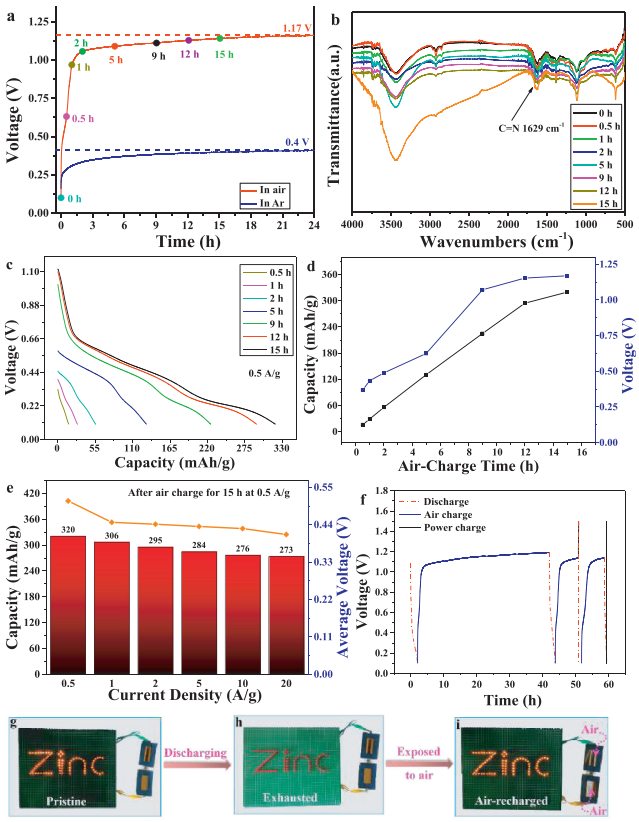

Fig. 4. (a) Charge curves of discharged flexible aqueous Zn//TNHATN batteries in air and Ar atmospheres. *Ex situ* FTIR spectra of the TNHATN-Zn-H electrode at the marked points in the air-recharge process. (b) Electrochemical properties of the air-rechargeable flexible aqueous Zn//TNHATN battery: (c) Galvanostatic discharge curves at different air-charging times at 0.5 A/g. (d) Dependence of discharge capacity and charge voltage on air-charging times. (e) Capacities and discharged voltages at various current densities. (f) Charging/discharging behavior in hybrid modes. (g–i) LED lights powered by two air-rechargeable flexible aqueous Zn//TNHATN batteries at different states.

charge capacities under different folding angles, it can be found that they remain basically unchanged (Fig. 3c and Fig. S20). The results show that the flexible battery has strong mechanical property along with excellent flexibility. Furthermore, a single flexible battery under flat/folding angle of 90° situation (Fig. S21 in Supporting information) could power a LED light lightening. Only two such flexible batteries in series can light up the pattern of 74 LEDs (zinc), as presented in Fig. 3d, displaying its application potential in wearable electronics.

It is well known that the occurrence of redox reaction is related to the redox potential difference (ΔE) between reactants. Based on the Nernst equation and the CV curves in Fig. 2a and Fig. S22 (Supporting information), the obtained H^+/Zn^{2+} extraction potential of the discharged TNHATN electrode (*vs.* standard hydrogen electrode (SHE)) is -0.2 V. Furthermore, the standard electrode potential of O_2 *versus* SHE in the alkaline medium is 0.40 V [16], therefore, the ΔE between the discharged TNHATN electrode (TNHATN-nZn-(12–2n)H, abbreviated as TNHATN-Zn-H) and O_2 is larger than zero (Fig. 1c), indicating the redox reaction between them can take place easily. To demonstrate the feasibility of this reaction used to construct an air-rechargeable organic AZIB, we investigated the redox behavior of the TNHATN-Zn-H electrode in an air atmosphere using the flexible aqueous Zn//TNHATN battery.

The charge voltages of the discharged flexible aqueous Zn//TNHATN battery under different time in air/Ar is displayed Fig. 4a. As shown in Fig. 4a, when the TNHATN-Zn-H electrode is exposed to air, the voltage of the flexible aqueous Zn//TNHATN battery rapidly increases within 2 h, then gradually increases and finally stabilizes at 1.17 V after 24 h. This reveals that the TNHATN-Zn-H electrode is oxidized by O_2 in air. Conversely, in an Ar atmosphere, the voltage of the flexible aqueous Zn//TNHATN battery increases only to 0.4 V from 0.17 V after 24 h. This change originates from the relaxation behavior of the electrode [21]. Various *ex-situ* tests, such as FT-IR, XRD and XPS, were used to further investigate the redox process of the TNHATN-Zn-H electrode in the air-recharging process. FT-IR spectra of the TNHATN-Zn-H electrode at different charge time points presented in Fig. 4b show that the intensity of the peak belonged to the C=N bond at around 1629 cm^{-1} increases with the increase of the air-charging time from 0 to 15 h, which indicates the removal of H^+ ions during oxidation. The *ex-situ* XRD patterns show that the peak at around $2\theta = 9.7°$ belonged to the (021) crystal plane of TNHATN moves to the larger angle with the extension of air oxidation time (Fig. S23 in Supporting information), meaning the inter-plane distance (*d*-spacing) decreases and the extraction of H^+ ions from the TNHATN-Zn-H electrode. In the same time, the peak belonged to the (211) crystal plane of TNHATN appears again with air oxidation time increases to 9 h, further demonstrating the extraction of H^+ ions. In the *ex-situ* XPS spectra (Figs. S24a and b in Supporting information), the peak intensity of C=N (399.7 eV) gradually increases as the oxidation time increases, the peaks intensities of −NH− (400.3 eV) and O−H (533.1 eV) gradually become smaller, while the peak intensity of N−Zn (399.0 eV) and O−Zn (531.6 eV) has almost no change, indicating that H^+ ions remove and Zn^{2+} ions do not remove during air-recharging. The XPS spectra of Zn^{2+} ions (Fig. S25a in Supporting information) and the *ex-situ* SEM-EDS mapping images (Fig. S25b in Supporting information) also further demonstrate the judgment mentioned above. As observed in Figs. S25 and S26 (Supporting information), the peaks intensities of Zn $2p_{3/2}$ and Zn $2p_{1/2}$ and the Zn element content at the fully discharged state almost increase slightly than that of the air-recharged for 15 h, which is attributed to that the extraction potential of Zn^{2+}ions (0.46 V *vs.* SHE, Fig. S22) is higher than the standard electrode potential (0.40 V *vs.* SHE) of O_2 in the alkaline medium. In other words, the oxidation reaction process of the discharged electrode with O_2 is almost only involved in H^+ ions removal. During this course, O_2 can be turned to OH^- ions by accepting electrons and reacting with H_2O. Based on the facts above mentioned, we speculate the possible cathode reaction mechanism in the air-recharging process is as follows:

$$\text{TNHATN-nZn-(12-2n)H} - (12\text{-}2n)H^+ - (12\text{-}2n)e^- \rightarrow \text{TNHATN-nZn} \quad (2)$$

$$(12\text{-}2n)/4\ O_2 + (12\text{-}2n)/2\ H_2O + (12\text{-}2n)e^- \rightarrow (12\text{-}2n)OH^- \quad (3)$$

$$(12\text{-}2n)H^+ + (12\text{-}2n)OH^- \rightarrow (12\text{-}2n)H_2O \quad (4)$$

The electrochemical performance of air-rechargeable flexible aqueous Zn//TNHATN batteries were investigated by a series of tests. The discharge capacity and voltage change of the air-rechargeable flexible aqueous Zn//TNHATN battery under different air-charging times was tested at 0.5 A/g (Figs. 4c and d). The Zn//TNHATN battery can deliver a discharge capacity of 131 mAh/g after oxidation of 5 h. When the air-charging time reaches 15 h, the discharge capacity of the Zn//TNHATN battery reaches 320 mAh/g, which is higher than that of many air-rechargeable AZIBs previously reported (Table S4 in Supporting information) [16–21].

As the air-charging time increases, the voltage of the Zn//TNHATN battery gradually rises. After 5 h oxidation, the Zn//TNHATN battery can be restored to 0.58 V. When the oxidation time is increased to 15 h, the voltage of the Zn//TNHATN battery

stabilizes at an open-circuit voltage of 1.17 V. After air-recharge for 15 h, such Zn//TNHATN batteries exhibit excellent rate performance (Fig. 4e and Fig. S27a in Supporting information), due to the fast insertion and removal of H^+ ions. The high discharge specific capacity of 273 mAh/g is maintained at a current density of 20 A/g, keeping 85.3% of that at 0.5 A/g. Furthermore, in the air environment, such flexible Zn//TNHATN batteries also have repeated self-rechargeability, as can be seen from the air-recharge/galvanostatic discharge cycle curves (Fig. S27b in Supporting information). On top of that, such flexible Zn//TNHATN batteries can switch freely between charge and discharge modes and operate well (Fig. 4f). After 7 h of air-charging (also known as chemical self-charge), the discharge voltage of Zn//TNHATN battery can maintain at about 1.14 V. When the energy in the Zn//TNHATN battery is depleted, it can be recharged again through air oxidation. Impressively, the Zn//TNHATN battery can be recharged by using an external power source, completing the transition from an air-recharged (1.14 V) state or a fully discharged (0.1 V) state to a fully charged state (1.5 V).

To verify practical application effects of the air-rechargeable flexible Zn//TNHATN batteries, two such pristine Zn//TNHATN batteries were assembled in series to power the LED lights, and they can light up 74 LED lights (Fig. 4g). After the Zn//TNHATN batteries were depleted (Fig. 4h), the sealing Kapton film was uncovered and air was introduced into the Zn//TNHATN batteries to achieve air-charging (Fig. 4i and Fig. S28 in Supporting information). Impressively, depleted Zn//TNHATN batteries can light up the LED lights again after air-charge, proving their viability as air self-charging energy storage devices.

In conclusion, we have successful developed a flexible AZIB with air-recharging capability based on the TNHATN cathode. The flexible aqueous Zn//TNHATN battery not only delivers high discharge capacity, but also exhibits high volumetric energy density (21.36 mWh/cm^3), good mechanical flexibility and better long cycle stability, owing to TNHATN having π-conjugated aromatic structure containing multiple redox active sites and electron-withdrawing groups. Impresively, such flexible aqueous Zn//TNHATN battery also shows excellent air-recharging capability. The discharged flexible aqueous Zn//TNHATN battery can be recharged to the open-circuit voltage of 1.17 V after oxidation in air for 15 h, then delivers a specific capacity of up to 320 mAh/g at 0.5 A/g. Due to the potential difference between the discharged TNHATN cathode and O_2, during the air-charging process, along with the removal of H^+ ions, the redox reaction between them can happen spontaneously. Notably, this flexible aqueous Zn//TNHATN battery also displays excelent rate performance and works well in chemical or/and galvanostatic charging mixed modes, showing reusability. To our best knowledge, this is the first report about the flexible air-rechargeable AZIBs based on organic cathodes with H^+ removal. This study provides a new insight for constructing high-capacity and flexible air-rechargeable AZIBs.

Declaration of competing interest

The authors declare that they have no known competing financial interests or personal relationships that could have appeared to influence the work reported in this paper.

Acknowledgments

This study was supported by the National Natural Science Foundation of China (No. 21975034), the Project Funded by the Priority Academic Program Development of Jiangsu Higher Education Institutions and the Research Project of State Key Laboratory of Coordination Chemistry. Thanks to the High Performance Computation Laboratory of Changzhou University and the institute of Theoretical Chemistry of Jilin University.

Supplementary materials

Supplementary material associated with this article can be found, in the online version, at doi:10.1016/j.cclet.2023.108487.

References

[1] D.L. Chao, W.H. Zhou, C. Ye, et al., Angew. Chem. Int. Ed. 58 (2019) 7823–7828.
[2] D. Bin, W. Huo, Y. Yuan, et al., Chem 6 (2020) 968–984.
[3] Y. Liu, Z. Pan, D. Tian, et al., Chem. Eng. J. 399 (2020) 125842.
[4] C. Li, X. Xie, H. Liu, et al., Nat. Sci. Rev. 9 (2022) nwab177.
[5] F. Wan, L. Zhang, X. Dai, et al., Nat. Commun. 9 (2018) 1656.
[6] Y.Q. Yang, Y. Tang, S.Q. Liang, et al., Nano Energy 61 (2019) 617–625.
[7] N. Zhang, F. Cheng, J. Liu, et al., Nat. Commun. 8 (2017) 405.
[8] F. Wan, Y. Zhang, L.L. Zhang, et al., Angew. Chem. Int. Ed. 58 (2019) 7062–7067.
[9] P. Yu, Y. Zeng, H. Zhang, et al., Small 15 (2019) 1804760.
[10] M. Narayanasamy, B. Balan, C. Yan, et al., Chin. Chem. Lett. 34 (2023) 108076.
[11] W. Yang, W. Yang, Y. Huang, et al., Chin. Chem. Lett. 33 (2022) 4628–4634.
[12] R. Huanga, W. Wang, C. Zhang, et al., Chin. Chem. Lett. 33 (2022) 3955–3960.
[13] X.L. Xie, Z.S. Fang, M.J. Yang, et al., Adv. Funct. Mater. 31 (2021) 2007942.
[14] P. Chen, T.T. Li, Y.B. Yang, et al., Nat. Commun. 13 (2022) 64.
[15] L.T. Ma, Y.W. Zhao, X.X. Ji, et al., Adv. Energy Mater. 9 (2019) 1900509.
[16] Y. Zhang, F. Wan, S. Huang, et al., Nat. Commun. 11 (2020) 2199.
[17] L. Yan, Y. Zhang, Z. Ni, et al., J. Am. Chem. Soc. 143 (2021) 15369–15377.
[18] C.Z. Liu, W.W. Xu, C.T. Mei, et al., Adv. Energy Mater. 11 (2021) 2003902.
[19] M. Liao, J.W. Wang, L. Ye, et al., J. Mater. Chem. A 9 (2021) 6811–6818.
[20] W.D. Qiu, Z.C. Lin, H.B. Xiao, et al., Mater. Adv. 2 (2021) 6694–6702.
[21] Z.W. Tie, Y. Zhang, J.C. Zhu, et al., J. Am. Chem. Soc. 144 (2022) 10301–10308.
[22] T. Sun, Z.J. Li, Y.F. Zhi, et al., Adv. Funct. Mater. 31 (2021) 2010049.
[23] K.W. Nam, H. Kim, Y. Beldjoudi, et al., J. Am. Chem. Soc. 142 (2020) 2541–2548.
[24] M. Na, Y. Oh, H.R. Byon, Chem. Mater. 32 (2020) 6990–6997.
[25] Y. Gao, G. Li, F. Wang, et al., Energy Storage Mater. 40 (2021) 31–40.
[26] Y. Zhang, Y. Liang, H. Dong, et al., J. Electrochem. Soc. 167 (2020) 070558.
[27] Y. Wang, C. Wang, Z. Ni, et al., Adv. Mater. 32 (2020) 2000338.
[28] J. Xie, F. Yu, J. Zhao, et al., Energy Storage Mater. 33 (2020) 283–289.
[29] D. Kundu, P. Oberholzer, C. Glaros, et al., Chem. Mater. 30 (2018) 3874–3881.
[30] Q. Zhao, W. Huang, Z. Luo, et al., Sci. Adv. 4 (2018) eaao1761.
[31] Z.W. Guo, Y.Y. Ma, X.L. Dong, et al., Angew. Chem. Int. Ed. 57 (2018) 11737–11741.
[32] G. Sun, B. Yang, X. Chen, et al., Chem. Eng. J. 431 (2022) 134253.
[33] Z. Ye, S. Xie, Z. Cao, et al., Energy Storage Mater. 37 (2021) 378–386.
[34] W. Wang, V.S. Kale, Z. Cao, et al., ACS Energy Lett. 5 (2020) 2256–2264.
[35] X.J. Chen, H.Q. Su, B.Z. Yang, et al., Sustain. Energy Fuels 6 (2022) 2523–2531.
[36] Z. Tie, L. Liu, S. Deng, et al., Angew. Chem. Int. Ed. 59 (2020) 4920–4924.
[37] Q. Wang, X. Xu, G. Yang, et al., Chem. Commun. 56 (2020) 11859–11862.
[38] X.D. Liu, Z.B. Ye, Adv. Energy Mater. 11 (2021) 2003281.
[39] S. Er, C. Suh, M.P. Marshak, et al., Chem. Sci. 6 (2015) 885–893.
[40] C.J. Xu, B.H. Li, H.D. Du, et al., Angew. Chem. Int. Ed. 51 (2012) 933–935.
[41] P. Simon, Y. Gogotsi, B. Dunn, Science 343 (2014) 1210–1211.
[42] H.L. Pan, Y.Y. Shao, P.F. Yan, et al., Nat. Energy 1 (2016) 16039.